

Climate variability in the Aral Sea basin (Central Asia) during the late Holocene based on vegetation changes

Philippe Sorrel^{a,*}, Speranta-Maria Popescu^b, Stefan Klotz^{b,c}, Jean-Pierre Suc^b, Hedi Oberhänsli^a

^a *GeoForschungsZentrum Potsdam, Telegraphenberg, D-14473 Potsdam, Germany*

^b *Laboratoire PaléoEnvironnements et PaléobioSphère (UMR 5125 CNRS), Université Claude Bernard-Lyon 1, 27–43 boulevard du 11 Novembre, F-69622 Villeurbanne Cedex, France*

^c *Institut für Geowissenschaften, Universität Tübingen, Sigwartstrasse 10, D-72070 Tübingen, Germany*

Received 21 November 2006

Available online 25 January 2007

Abstract

High-resolution pollen analyses (~50 yr) from sediment cores retrieved at Chernyshov Bay in the NW Large Aral Sea record shifts in vegetational development from subdesertic to steppe vegetation in the Aral Sea basin during the late Holocene. Using pollen data to quantify climatic parameters, we reconstruct and date for the first time significant changes in moisture conditions in Central Asia during the past 2000 yr. Cold and arid conditions prevailed between ca. AD 0 and 400, AD 900 and 1150, and AD 1500 and 1650 with the extension of xeric vegetation dominated by steppe elements. These intervals are characterized by low winter and summer mean temperatures and low mean annual precipitation ($P_{\text{mm}} < 250$ mm/yr). Conversely, the most suitable climate conditions occurred between ca. AD 400 and 900, and AD 1150 and 1450, when steppe vegetation was enriched by plants requiring moister conditions ($P_{\text{mm}} \sim 250$ –500 mm/yr) and some trees developed. Our results are fairly consistent with other late Holocene records from the eastern Mediterranean region and the Middle East, showing that regional rainfall in Central Asia is predominantly controlled by the eastern Mediterranean cyclonic system when the North Atlantic Oscillation (NAO) is in a negative phase. © 2006 University of Washington. All rights reserved.

Keywords: Pollen analysis; Vegetation; Climate; Aral Sea; Late Holocene; Central Asia; Negative NAO

Introduction

Numerous biostratigraphic, geomorphological and archaeological proxy data document that climate of Central Asian deserts and semi-deserts experienced many changes at various time scales through the Pleistocene and Holocene (e.g., Velichko, 1989; Tarasov et al., 1998a; Boomer et al., 2000; Boroffka et al., 2005, 2006). Climatic variations resulted in multiple shifts from hyper-arid to semi-arid deserts and even steppe vegetations with development of shrubs (Kremenetski and Tarasov, 1997; Kremenetski et al., 1997; Tarasov, 1992; Tarasov et al., 1997, 1998a). Whereas environmental and climate changes are well documented in southwestern Siberia

and Kazakhstan during the Pleistocene and early Holocene (Kremenetski and Tarasov, 1997; Kremenetski et al., 1997; Tarasov et al., 1997), however, they are still scarce for the Aral Sea (e.g., Rubanov et al., 1987; Boomer et al., 2000). Using pollen and tree macrofossil records, Tarasov et al. (1998a) reconstructed vegetation biomes at ca. 6000 ¹⁴C yr BP and documented dry conditions similar to present-day ones around the Aral Sea. Distinct vegetation changes occurred in north-eastern Kazakhstan (Kremenetski and Tarasov, 1997). From two peatlands and two lakes sections, they document a milder climate between 6000 and 4500 ¹⁴C yr BP, followed by drier and more continental conditions during 4500–3600 ¹⁴C yr BP, and a “less continental” climate during 3300–2700 ¹⁴C yr BP. Recently, Esper et al. (2002) published a high-resolution climate record from the Karakorum and Tien-Shan Mountains based on tree-ring width, documenting prominent temperature changes for the last 1200 yr. They reported relatively warm conditions during AD 800–1000, AD 1300–

* Corresponding author. Present address: Laboratoire « Morphodynamique continentale et côtière (M2C) » (UMR 6143 CNRS), Université de Caen Basse-Normandie, 24 rue des Tilleuls, F-14000 Caen, France. Fax: +33 231 565 757.

E-mail address: philippe.sorrel@unicaen.fr (P. Sorrel).

1450, and during the past century. In contrast, lowered temperatures were inferred during AD 1000–1200 and during the “Little Ice Age” (AD 1450–1900).

In the Aral Sea area, high-resolution climatic studies have been recently undertaken in the context of the project CLIMAN (Nourgaliev et al., 2003; Sorrel et al., 2006). In this study, we present a new pollen record covering the last 2000 yr with a time resolution of ca. 50 yr. Based on quantitative pollen analyses, we use pollen data to show significant changes in moisture conditions, temperature, and vegetation patterns in the Aral Sea basin. Our objective is to identify climatically induced shifts in the terrestrial vegetation surrounding the lake and to compare them to other records from the Middle East and Central Asia. These data are then critically evaluated in order to initially assess late Holocene climatic changes in Central Asia.

Geological and climatic frame of the Aral Sea basin

The Aral Sea, situated in Central Asia (Fig. 1), represents an ideal sedimentary archive for studying environmental and climate changes in the past. The present-day climate is marked by extreme continental conditions that are mediated by a complex topography around the Aral Sea. The Central Asian arid region (=Aral Sea basin) comprises the Turan Lowland and the Kyzyl Kum, and it is surrounded in the north by the southern margin of the Kazakh Hills (at ca. 48°N), the Middle Asian Mountains on its southern and southeastern edges (Pamir, Tien Shan), and the lower mountains of the Kopet Dagh (2000 m altitude) in the southwest (Fig. 1). In the north, the Turan Lowland descends progressively northward and westward and opens towards the Caspian lowland (Lioubimtseva et al., 2005). In the Aral Sea basin, ecosystems mostly represented by steppes (including shrubs) are the



Figure 1. Location map of the Aral Sea and the study area (modified after Lioubimtseva et al., 2005).

prevailing landscapes. Some isolated trees (e.g., poplar, tamarisk, elm, oak), which are typical for riparian ecosystems, are restricted to the banks of two major Central Asian rivers, the Syr Darya and the Amu Darya. Winters, dominated by the Siberian High Pressure Cell (Zavialov, 2005), are cold. Severe frosts, with mean temperatures of $-26\text{ }^{\circ}\text{C}$ and absolute minimum of $-40\text{ }^{\circ}\text{C}$ are common (Lioubimtseva et al., 2005). In contrast, summers are hot, cloudless and dry. In autumn, a rapid cooling of the land tends to stabilize the atmosphere, protracting the dry season. Therefore, rain is rare in the basin with maximum precipitation in winter and early spring (Lioubimtseva, 2002; Nezhlin et al., 2005), whereas almost no rain occurs between May and October (e.g., Létolle and Mainguet, 1993; Zavialov, 2005). Overall, the characteristic number of rainy days is 30–45 per yr (Bortnik and Chistyayeva, 1990), and precipitation over the Aral Sea tends to increase northwards (Zavialov, 2005).

Materials and methods

Site, sediments and chronology

During a field campaign in the summer 2002, piston cores CH1 (11.04 m) and CH2 (6.0 m) ($45^{\circ}58.528'\text{N}$, $59^{\circ}14.459'\text{E}$; water depth 22 m) were retrieved with a Usinger piston corer (<http://www.uwitec.at>) about one km off the shoreline at Chernyshov Bay (Fig. 1). We investigated the composite

sediment core CH2/1 (Cores CH1 and CH2), whose total length is 10.79 m. The correlation between Cores CH1 and CH2 was performed by matching laminations, using photographs, physical properties and XRF scanning data. Detailed lithological description of section CH2/1 is given in Sorrel et al. (2006). A simplified lithological profile and the age model for section CH2/1 are presented in Figure 2.

In section CH2/1, reliable dating for the upper 5 m was obtained by correlation with the magnetic susceptibility record from parallel cores 7, 8 and 9 retrieved ca. 50 m apart from the studied cores (Nourgaliev et al., 2003). This correlation provides an age of 480 ± 120 cal yr BP at 1.4 m depth and 655 ± 65 cal yr BP at 4.48 m in section CH2/1 (Table 1). For the lower part of section CH2/1 [5.00–10.79 m], AMS radiocarbon ages were determined using the green alga *Vaucheria* sp. and CaCO_3 from mollusc shells, which were successively picked from the washed sediment sample and carefully cleaned from adhering particles. Algae were stored in distilled water within a glass vessel. For each sample, AMS ^{14}C dating was performed using between 0.2 and 1.0 mg of pure extracted carbon. Extrapolation of sedimentation rates below 8.3 m provides an age of ca. 2000 ^{14}C yr BP for the basement of section CH2/1. A sampling interval of 30 to 40 cm was selected, which provides a time resolution of ca. 50 yr. The top of the core (uppermost 40 cm) has been dated as post-AD 1963, as based on a peak in ^{137}Cs at 0.46 m reflecting the bomb period (ca. AD 1963–1964) (Heim,

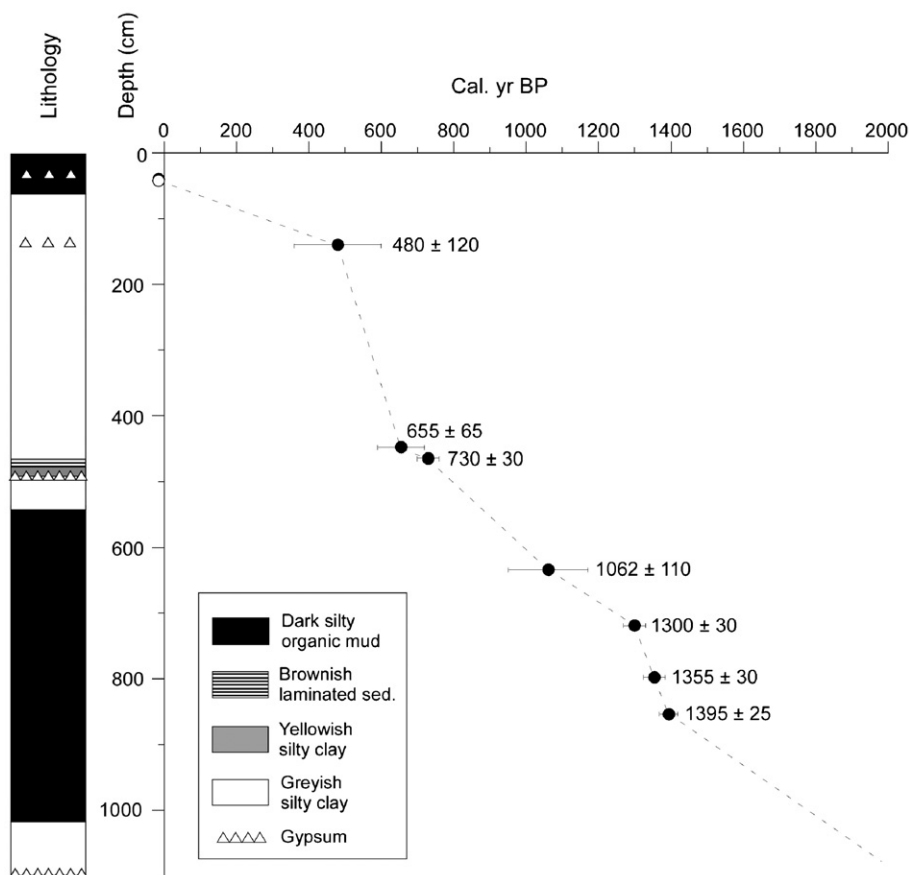


Figure 2. Simplified lithological profile and age model for section CH2/1 based on AMS ^{14}C dating (full dots). Open dot: peak in ^{137}Cs [AD 1963–1964].

Table 1
Radiocarbon dates for section CH2/1. AMS ^{14}C ages were measured at Poznań Radiocarbon Laboratory (Poland)

Sample name	Core depth (m)	Lab. no.	^{14}C yr BP	2 Std. dev. (95% confidence interval)	cal. yr BP	Dated material
Nourgaliev et al. (2003) ¹	1.4	KSU 2	435	120	480	<i>Vaucheria</i> sp.
Nourgaliev et al. (2003) ²	4.48	KSU 3	640	65	655	<i>Vaucheria</i> sp.
Aral 32 134.5–138.5 cm	4.65	Poz-13511	815	30	730	TOC
Aral 27 209–212 cm	6.34	Poz-12279	1160	110	1062	<i>Vaucheria</i> sp.
Aral 27 269–271 cm	6.93	Poz-4762	1395	30	1300	<i>Vaucheria</i> sp.
Aral 28 40–45; 52–54 cm	~7.73	Poz-9662	1480	30	1355	molluscs
Aral 28 112–114 cm	8.28	Poz-4760	1515	25	1395	<i>Vaucheria</i> sp.

Radiocarbon ages were corrected to calibrated (cal) ages using the IntCal04 calibration curve (Reimer et al., 2004).

2005). Our age model is very similar to that established on Core CH1 for the diatom-inferred palaeoconductivity record of Austin et al. (2007). It diverges only on a few points and these discrepancies are mostly due to the fact that: (1) different cores from Chernyshov Bay were investigated, i.e., Core CH1 in Austin et al. (2007) and section CH2/1 in this study; (2) different calibration methods were used, i.e., OxCal v. 3.10 (Bronk Ramsey, 2005) in Austin et al. (2007) whereas the IntCal04 calibration curve (Reimer et al., 2004) has been used here. However, the source of the ^{14}C dating remains the same (project CLIMAN; <http://climan.gfz-potsdam.de/>). For further detail on the chronology of section CH2/1, we refer to Sorrel et al. (2006).

Sample processing

Pollen slide preparation followed the Cour's method (Cour, 1974). 35 sediment samples (15–25 g dry weight) were treated with cold HCl (35%) and cold HF (70%) to remove carbonates and silicates. Denser particles were separated from the organic residue using ZnCl_2 (density=2.0). Residues were filtered through a 150- μm nylon sieve to eliminate the coarser particles including organic macroremains. Palynomorphs were further concentrated using a 10- μm nylon sieve after a brief sonication (about 30 s). The final residue was then homogenized, and mounted onto microscope slides with glycerol. A transmitting light microscope using 400 \times and 1000 \times magnifications was used for pollen identification. Pollen identification was performed using the pollen photograph bank and several atlases of the 'Laboratoire PaléoEnvironnements et PaléobioSphère' (Lyon) as well as its pollen database, "Photopal" (<http://medias.obs-mip.fr/photopal>). Pollen grains are very well preserved in late Holocene sediments from section CH2/1 and abundant in all samples. Pollen concentration was estimated using the Cour's method (Cour, 1974). Concentration in palynomorphs varies from <500 to >45,000 grains/g. Pollen zones were assessed using a canonical correspondence analysis performed on selected taxa representing variables. Pollen enumeration was conducted at the Laboratory 'PaléoEnvironnements et PaléobioSphère', and data are stored in the C.P.C. database (<http://cpc.mediasfrance.org>).

Taxonomy and ecological grouping of pollen grains

Since pollen grains found in modern sediments and transported either by air or by rivers reflect the local to regional

vegetation, we used the botanical determination of pollen grains to reconstruct palaeovegetation in the Aral Sea basin. A minimum of 100 pollen grains, excluding Amaranthaceae–Chenopodiaceae and *Artemisia*, which are usually over-represented in arid environments, and non-determinable (i.e., poorly preserved) pollen grains, were counted in each sample. Generally more than 25 different taxa were found in each sample. 74 taxa have been identified (Table 2), and 17,356 pollen grains were enumerated.

Two different diagrams were developed from these data:

- A detailed pollen diagram (Fig. 3) displays percentages of the most frequent taxa, which were calculated relative to the total pollen sum;
- A standard synthetic diagram (Fig. 4), in which pollen taxa are represented in 10 relevant groups of taxa based on their ecological preferences (Table 2), to visualize changes in the vegetation pattern (composition, structure).

Climate reconstruction

For the quantification of palaeoclimate signals recorded in plant assemblages, the "probability mutual climatic spheres" (PCS) method described in detail by Klotz and Pross (1999) and Klotz et al. (2003, 2004) was favoured over modern analogue methods (e.g., Guiot, 1987, 1990; Prentice et al., 1992, 1996; Peyron et al., 1998; Tarasov et al., 1998a,b; Klotz, 1999). Generally, modern analogue methods (MAM) are based primarily on comparing past pollen spectra with present-day analogues. In this study, the main restriction in applying this technique is the general poorness of the underlying available database of surface pollen spectra from the Aral Sea region (only 91 in Kazakhstan; Tarasov et al., 1998a) that could serve as modern analogues for reliable climate reconstructions. Besides, the usefulness of these methods is restricted when no present-day analogues exist for past pollen floras, as is the case for the association Amaranthaceae–*Artemisia*–*Taxodium* found in this record. In addition, climate reconstructions with modern analogue methods may be significantly influenced by taphonomic effects when applied, for instance, on records from areas such as the Aral Sea basin, which experiences numerous dust storms throughout the year (Seredkina, 1960; Létolle and Mainguet, 1993; Zvialev, 2005). Hence, the use of the PCS method is more suitable than MAM for reconstructing climate changes in this study.

Table 2

List of the taxa identified within section CH2/1

Mega-mesothermic (=subtropical) elements	<i>Pterocarya</i>	<i>Rumex</i>
<i>Engelhardia</i>	<i>Eucommia ulmoides</i>	<i>Polygonum</i>
<i>Myrica</i>		Caryophyllaceae
Taxodiaceae (including <i>Taxodium</i> -type)	Meso-microthermic (=mid-latitude) elements	<i>Phlomis</i>
	<i>Tsuga</i>	Cyperaceae
Other mega-mesothermic elements:	<i>Cathaya</i>	
<i>Nyssa</i>		Other herbs:
<i>Mappianthus</i>	Microthermic (=high-latitude) elements	Asteraceae Cichorioideae type
Euphorbiaceae	<i>Abies</i>	<i>Polygonum</i>
		<i>Gallium</i>
Mesothermic (=warm temperate) elements	<i>Pinus</i>	Cannabaceae
<i>Quercus</i>		Fabaceae
<i>Alnus</i>	Schlerophyllous elements	Plumbaginaceae
<i>Liquidambar</i>	Cupressaceae	<i>Urtica</i>
<i>Juglans</i>	evergreen <i>Quercus</i>	Zygophyllaceae
<i>Ulmus</i>		Brassicaceae
<i>Carpinus</i>	Aquatic plants	<i>Helianthemum</i>
<i>Populus</i>	<i>Sparganium</i> + <i>Typha</i>	Geraniaceae
<i>Betula</i>	<i>Potamogeton</i>	<i>Sambucus</i>
<i>Corylus</i>		Papaveraceae
Other mesothermic elements:	Other aquatic plants:	<i>Plantago</i>
<i>Buxus sempervirens</i> type	<i>Myriophyllum</i>	Apiaceae
<i>Vitis</i>	<i>Aristolochia</i>	Ericaceae
<i>Juglans cf. cathayensis</i>	<i>Alisma</i>	Liliaceae
<i>Zelkova</i>	<i>Nymphaea</i>	<i>Narcissus</i>
<i>Tilia</i>		
<i>Taxus</i>	Non-significant (=cosmopolitan) elements	<i>Calligonum</i>
<i>Salix</i>	Rosaceae	<i>Nitraria</i>
<i>Fagus</i>	Ranunculaceae	<i>Ziziphus spina-christi</i>
<i>Platanus</i>		
<i>Fraxinus</i>	Herbs	Steppe elements
<i>Acer</i>	Amaranthaceae–Chenopodiaceae	<i>Artemisia</i>
<i>Carya</i>	Asteraceae Asteroidae	<i>Ephedra</i>
	Poaceae	

Taxa are grouped according to their ecological requirements. The different groups are plotted in the synthetic pollen diagram.

The PCS method is independent of relative proportions of plants, considering only their presence (at a minimum level of 0.5% abundance). Generally, “mutual climatic range” methods (including the PCS) determine the climatic tolerance of past taxa by means of mutual present-day ranges of the climatic tolerances of the nearest living relatives (NLR) of the taxa represented in the past assemblages. It has been recognized a considerable advantage of this reconstruction method to be independent from the availability of modern analogues and from taphonomic influences (Mosbrugger and Utescher, 1997). Especially, the PCS method calculates probability intervals within the mutual climatic spheres by comparison with the spheres calculated for a multitude of present-day floras. These probability intervals result from the observation that the climatic preferences of the present-day floras are considerably restricted as compared to their potential range.

The quality of PCS has been tested on the basis of a multitude of present-day floras (Klotz et al., 2003, 2004) documenting the large agreement between reconstructed and actual grid climate values, with correlation coefficients and mean average error of 0.95 and 1.1 °C for summer temperatures, 0.95 and 1.7 °C for winter temperatures, 0.95 and 1.1 °C for mean annual

temperature and 0.86 and 100 mm for mean annual precipitation. Therefore, the PCS is considered to represent a very sensitive method for the interpretation of climate variability.

Results

Five ecostratigraphic pollen zones have been distinguished based on major changes in pollen assemblages, labelled as P1 to P5 (Figs. 3 and 4).

Pollen zone P1 (10.75–9.97 m; ca. AD 0–400)

This zone is characterized by a large supremacy of herbs (45–47.6%), mainly represented by Amaranthaceae–Chenopodiaceae (35–40%) and steppe elements (43–47%), with frequencies of *Artemisia* fluctuating between 42.7 and 46.8%. Among other herbaceous plants (Caryophyllaceae, Asteraceae Asteroidae, *Rumex*, Cyperaceae), Poaceae are abundant with values increasing towards the top (2.5–5.8%). Conversely, arboreal taxa are extremely rare (mega-mesothermic elements: <2%, mesothermic elements: <5%), mostly represented by Taxodiaceae (1.2% at 9.97 m), *Betula* (1.2% at 9.97 m) and few *Alnus* (<1%). Pollen grains of *Quercus*, *Carpinus*, *Populus*,

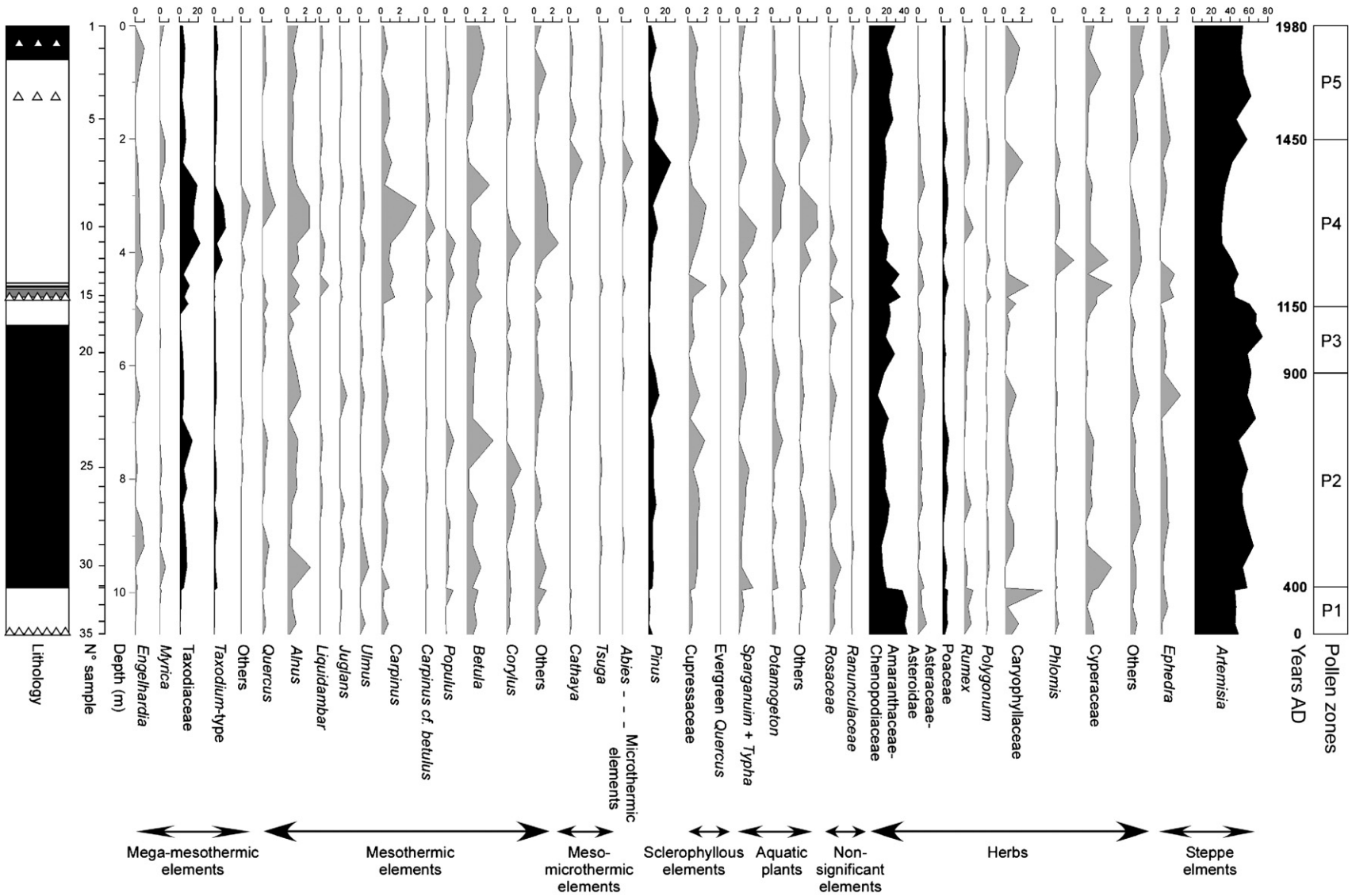


Figure 3. Pollen detailed diagram for section CH2/1. Black-filled lines indicate percentage abundance and gray-filled lines give 10× exaggeration (i.e., per mill abundance). Pollen zones P1 to P5 are based on the present study. For lithology, see Figure 2.

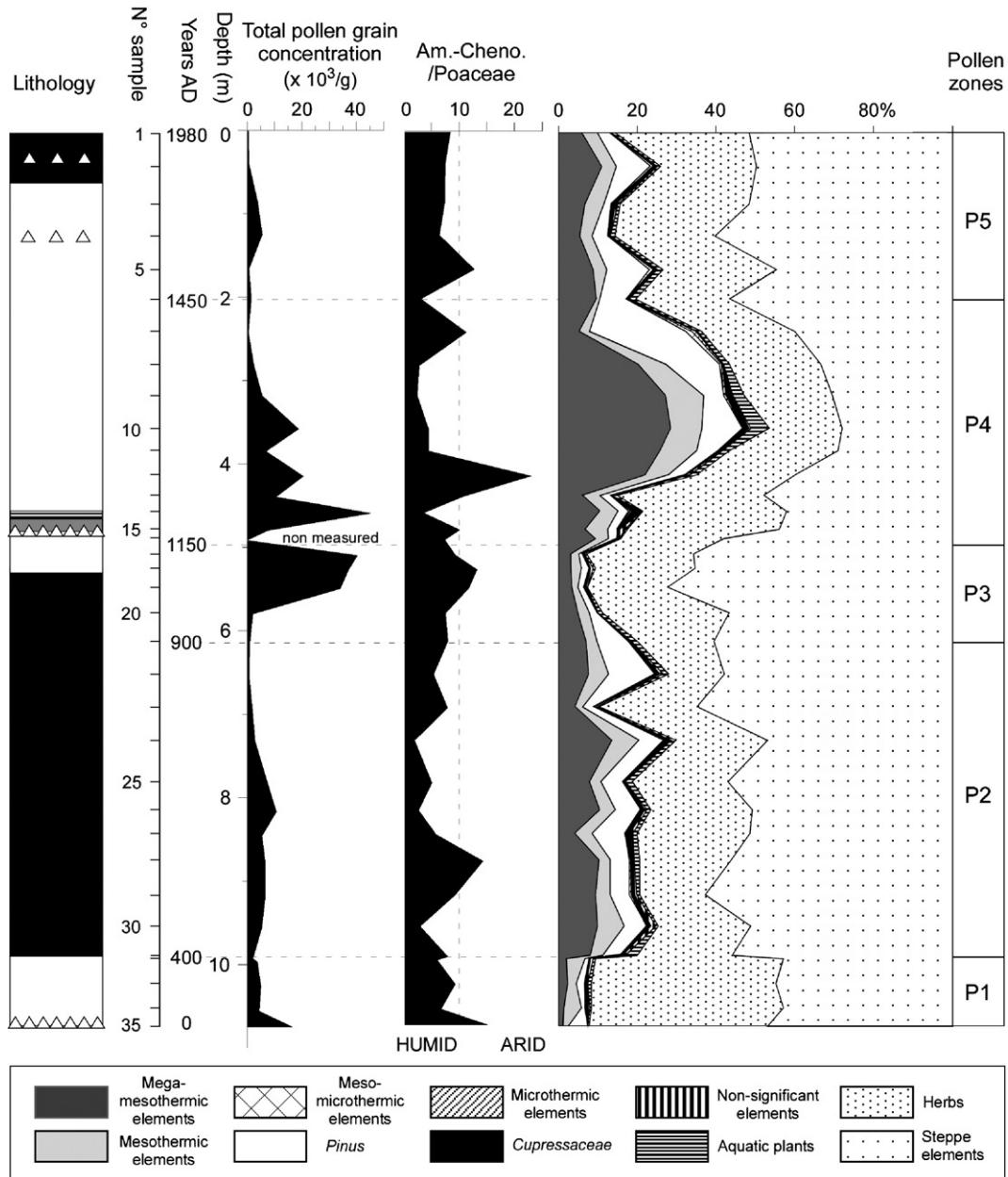


Figure 4. Pollen synthetic diagram for section CH2/1. Grouping was performed with regard to the ecology of the plants (see Table 2). Concentrations (per gram of dry sediment) are relative to the total pollen sum. Each sample represents a 30- to 40-cm interval and is plotted by its mean depth (see text for details). The ratio Amaranthaceae–Chenopodiaceae/Poaceae is regarded as representing a semi-quantitative index of aridity. For lithology, see Figure 2.

Corylus and Cupressaceae are also present at low percentages, with values never exceeding 1%. *Pinus* is found at low abundances (<5%), as are pollen of Rosaceae and aquatic plants (>1%). Total pollen concentration is relatively high in the lowermost part of this zone (16,600 grains/g at 10.75 m) but decrease upwards (<4000 grains/g at 9.97 m) (Fig. 4).

Pollen zone P2 (9.97–6.13 m; ca. AD 400–900)

This zone shows a conspicuous increase in percentages of arboreal taxa characterized by higher abundances of mega-mesothermic (Taxodiaceae: 13.3% at 7.33 m) and mesothermic (6.8% at 7.33 m) elements. Among other warm-temperate trees,

Betula, *Alnus* and *Corylus* are most abundant (Figs. 3 and 4). Frequency of Cupressaceae also slightly increases (1.7% at 7.33 m), while values of *Pinus* become more important (mean: 6.2%; 11.7% at 6.53 m). This zone is also characterized by a drastic decrease in percentages of Amaranthaceae–Chenopodiaceae (9–21%), and numbers of Poaceae also slightly decrease. Relative abundances of *Artemisia* (steppe) remain stable at relative high levels, even showing higher values than in zone P1 (47–65%). Non-significant pollen grains are also present in low values (<1.5%) and abundance of aquatic plants slightly increases (0.6–3%). Total pollen concentration is lower in this zone and fluctuates between 2000 and 10,500 grains/g (Fig. 4).

Pollen zone P3 (6.13–4.92 m; ca. AD 900–1150)

This zone is characterized by a general decrease in mega-mesothermic and mesothermic elements, with respective values of 2.8–9% and 1.5–3.4% (Fig. 4). In particular, abundances of Taxodiaceae (mean: 3.1%) and *Taxodium*-type (0–1.6%) show pronounced lower values compared to the previous zone. Among the mesothermic elements, *Alnus*, *Betula* and to a lesser extent *Quercus* and *Carpinus* are the most represented taxa, with values rarely exceeding 1%. Though frequencies of herbs (Amaranthaceae–Chenopodiaceae, Asteraceae Asteroidae, *Rumex*, *Phlomis*, Cyperaceae) remain stable compared to zone P2 (19.5–32%) with a slight decrease in Poaceae (1.5–3.6%), abundance of steppe elements conspicuously increases through elevated frequency of *Artemisia* (56–72%). Percentages of Cupressaceae, non-significant elements and aquatic plants are again relatively low (<2%), while *Pinus* frequency clearly decreases (mean: 2.7%). Total pollen concentration increases towards the top of this zone, with a maximum value of 40,000 grains/g at 5.1 m (Fig. 4).

Pollen zone P4 (4.92–2.02 m; ca. AD 1150–1450)

Following the increase in steppe elements in zone P3, this zone emphasizes a pronounced increase in percentages of trees and notably of mega-mesothermic elements with a maximum of 28.3% at 3.58 m (Figs. 3 and 4). Noticeably, relative abundances of Taxodiaceae fluctuate between 5% in the lowermost part of the zone (4.8 m) up to 21.7% at 3.85 m, while maximal values of *Taxodium*-type (12.2%) are recorded at 3.58 m. Pollen of *Engelhardia* and *Myrica* is also found but in low numbers (<1%), while rare specimens of *Nyssa* and *Mappianthus* have been recorded as well. Mesothermic elements are common (3.5–9.8%) and mostly represented, among other warm-temperate taxa, by *Carpinus* (3.7% at 3.18 m), *Alnus* (2.35% at 3.58 m), *Quercus* (1.4% at 3.18 m), *Betula* (1.15% at 3.85 m) and *Corylus* (1.5% at 3.85 m). *Populus* ($\leq 1\%$) and higher frequency of *Liquidambar* (<1%) also occur in this zone. *Pinus* becomes more abundant upwards, with a maximum of 24.3% at 2.42 m, while few pollen grains of *Tsuga* and *Abies* also have been found. Though frequency of Poaceae noticeably increases (6.5% at 4.59 m, 6% at 3.18 m; 5.6% at 2.82 m), as do values of Cyperaceae (0.2–2.8%), percentages of *Artemisia* conspicuously drop, with a minimum of 28.3% at 3.58 m and with values fluctuating around 40% throughout the zone. Abundances of Amaranthaceae–Chenopodiaceae are relatively similar as in zones P2 and P3 (14.8–32%). Aquatic plants increase noticeably (4.7% at 3.58 m), as does Cupressaceae (1.9% at 4.59 m). Total pollen concentration decreases in this zone from 45,000 grains/g at 4.59 m to less than 500 at 2.42 m (Fig. 4).

Pollen zone P5 (2.02–0.00 m; ca. AD 1450–1980)

This zone is characterized by the transition to present-day vegetation types, with an abrupt decrease in percentages of mega-mesothermic elements (5.15–10.6%) and to a lesser

extent of warm temperate trees (1–4.8%), correlative with an increase in herbs (23.8–33.6%) and steppe (45% to ca. 52% at the top) frequencies (Figs. 3 and 4). Mega-mesothermic elements are mainly represented by Taxodiaceae (including *Taxodium*-type) that nonetheless never exceed 10%, while other taxa from this group become scarce. Among the mesothermic elements, only abundance of *Betula* regularly exceeds 1%, whereas *Quercus*, *Alnus*, *Liquidambar*, *Populus* and *Corylus* mostly run below 1%. Percentages of Cupressaceae slightly decrease (0.2–1.1%), as does *Pinus* from 10.8% at 1.66 m to 3% at the top. *Tsuga*, *Abies* and non-significant elements still occur, but at very low numbers (<1%). Although Amaranthaceae–Chenopodiaceae yield a pronounced increase in this zone (16.7–27.7%), the frequency of Poaceae decreases (2–5.3%). Total pollen concentration is relatively low in this zone (<500–5550 grains/g) (Fig. 4).

Vegetation patterns derived from the pollen record

Herbs, predominant in all samples (Fig. 4), are characterized by an overwhelming presence of *Artemisia* that accounts for 28–72% of the pollen sum, and pollen of Amaranthaceae–Chenopodiaceae (20–25%). Poaceae (mean: 3.5%) is also common. Studies of pollen composition in aerosols indicate that both *Artemisia* and Amaranthaceae–Chenopodiaceae are high pollen producers (Van Campo et al., 1996; Cour et al., 1999), whereas Poaceae are rare in arid regions (Cour and Duzer, 1978; Van Campo et al., 1996). At present in Central Asia, *Artemisia* and Amaranthaceae–Chenopodiaceae are characteristic elements of steppe, semi-desert and desert environments (Tarasov et al., 1998a,b). Since Amaranthaceae–Chenopodiaceae are commonly present under saline and desert conditions but can be easily replaced, even during periods of minor elevation in precipitation, a slight increase in abundance can be interpreted as an increase in salinity and/or aridification (El Moslimany, 1990).

Pollen data suggest that open vegetation types with typical steppe elements (shrubs, herbs) were always predominant in the Aral Sea basin during the last 2000 yr. This implies that xeric conditions prevailed in the region, interrupted by periods of slightly enhanced moisture as reflected by slightly increased values of Poaceae. Based on the above ecological significance of Amaranthaceae–Chenopodiaceae (indicative of dry conditions) and Poaceae, whose abundance generally increases with rain, we use the ratio Amaranthaceae–Chenopodiaceae/Poaceae as a semi-quantitative index of aridity (Fig. 4). In this diagram, high values of the ratio (>10) are considered indicative of arid conditions that favour semi-desert-steppe vegetation, whereas low values (<10) reflect periods of slightly elevated moisture conditions and the development of few trees in a less arid steppe. This is concurrent with abundance of aquatic plants and Cyperaceae, which reflect some extension in aquatic environment (Fig. 3). Therefore, correspondence between low ratio values, sedimentological data and changes in lake water levels (Sorrel et al., 2006) validate the use of the ratio as a proxy for relative moisture availability in the Aral Sea basin.

Halophytes (Amaranthaceae–Chenopodiaceae, *Ephedra*, partly *Artemisia*) probably contribute to the predominant vegetation along the Aral Sea shoreline. However, the presence of aquatic plants is also common in the pollen flora. In general, frequency of aquatic plants is almost parallel to that of Poaceae (Fig. 3). Increasing frequency of these taxa may be thus representative of some extension of local marshes accompanied by some development of herbs requiring less dry conditions, reflecting a slight increase in humidity.

Trees are a minor component of the pollen flora, averaging 20% on the whole downcore, with a maximum value of 28% in zone P4. Each arboreal group is indicative of specific environmental conditions, permitting us to trace the probable origin of each taxon according to its ecology and present-day distribution. *Pinus* was probably not an eminent component of the regional vegetation; its frequency, even being modest, may be caused by its prolific production and overabundance in air and water transport. Warm-temperate elements (2–10%), also common in the pollen record, comprise some elements today restricted to the Middle East, such as *Liquidambar* and *Pterocarya*. The presence of these mesothermic elements may reflect the past development of some riparian vegetation in the Aral Sea basin. More surprisingly, in a region where such dry climate conditions predominated (judging from the overwhelming dominance of herbs in the pollen record), some mega-mesothermic elements indicative of relatively warmer and wetter environments have been found in every sample analysed. These elements are mostly represented by Taxodiaceae (including the *Taxodium*-type pollen, a swamp element) and to a lesser extent by *Engelhardia* and *Myrica*. Considering the regional, near sub-arid conditions in the basin during the last 2000 yr, the presence of these relictuous elements in the Aral Sea sediments requires comment. Similarly, the presence of *Cathaya* (a past conifer restricted today in a few mid-altitude environments of the southwestern subtropical China) among the mid-altitude elements would be unexpected in such conditions.

Because the Aral Sea is surrounded by older deposits mostly of Paleogene and Neogene age, we might expect increased reworking of older material from shore during periods of sheet wash erosion, as it is the case for dinoflagellate cysts (see Fig. 6). However, from several samples of Miocene marls collected nearby the Chernyshov Bay, no pollen grains of *Taxodium*-type, Taxodiaceae, *Cathaya*, *Engelhardia*, *Myrica* were found. On the contrary, in section CH2/1, most of these pollen grains are found well preserved, rarely broken or damaged, and exhibit all the criteria characteristic of fresh pollens. For further reliability, we carefully examined them under fluorescence light, a method that is currently used by palynologists to distinguish fresh from reworked specimens. Results showed that the pollen grains of *Cathaya*, *Taxodium*-type and other relictuous taxa display whitish to yellow tints that are usually characteristic of non-reworked pollen grains (unpublished data). Similar observations resulted from tests conducted on *Artemisia* and pollen grains of Amaranthaceae–Chenopodiaceae. Hence, the presence of mesothermic and mega-mesothermic relictuous taxa in sediments from Chernyshov

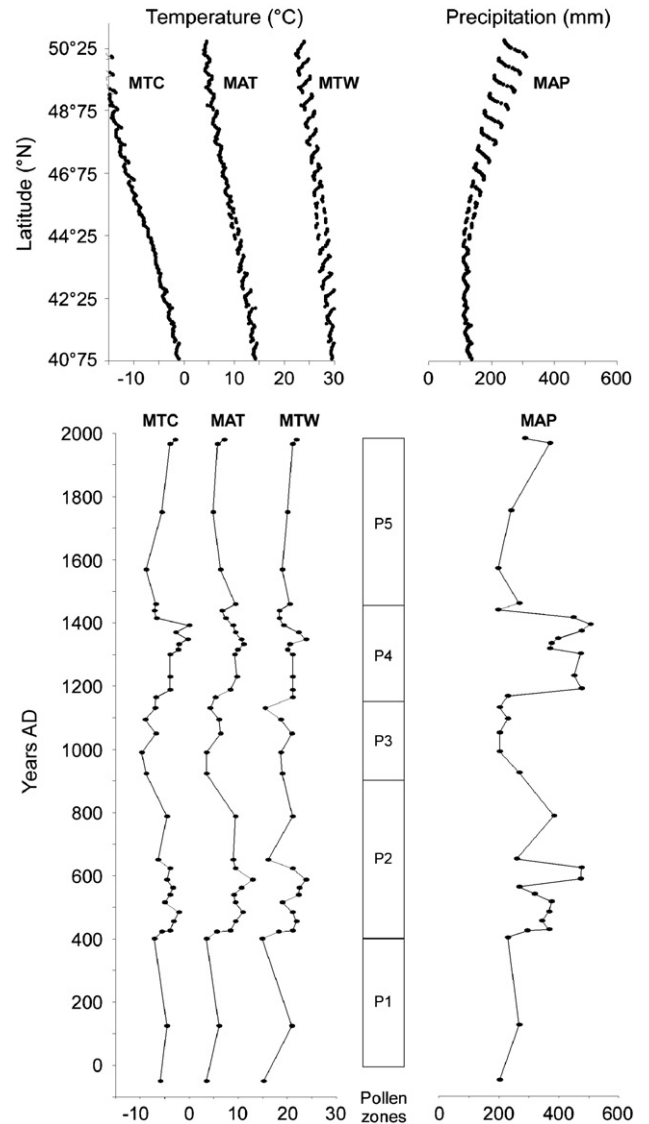


Figure 5. Reconstructed climate parameters: mean annual temperature (MAT in °C), mean temperature of the coldest month (MTC in °C), mean temperature of the warmest month (MTW in °C) and mean annual precipitation (MAP in mm/yr) for section CH2/1 during the last 2000 yr (lower diagram). Taxodiaceae and *Taxodium*-type have not been included for climate quantification (see text for detail). The upper figure represents instrumental data for present-day different temperature parameters, and mean annual precipitation in Central Asia. Data have been plotted along the latitudinal gradient [40°75′–50°25′N] (y). Data were extracted from New et al. (1999).

Bay is probably linked with mid- to long-distance wind transport, respectively.

Climate reconstruction

The composite pollen diagram (Fig. 4) suggests that some limited but significant changes in the vegetation pattern have occurred in the Aral Sea basin over the last 2000 yr. Changes in the pollen flora document switches between sub-desertic conditions (steppe almost completely constituted of *Artemisia*) and less dry environments (steppe enriched in Poaceae) coeval

to the establishment of some riparian trees. Since the expansion of open vegetation and the development of trees are controlled by climate conditions, we used the pollen data to reconstruct climate variability in terms of different temperature parameters and mean annual precipitation during the last 2000 yr (Fig. 5). For the climate reconstruction, all taxa recorded in samples from section CH2/1 have been included with the exception of Taxodiaceae. Indeed, *Taxodium* is naturally found today only in very restricted regions of southeast Asia, making the derived climatic sphere (e.g., coldest and warmest spheres of the species and their relationship) based on its geographical distribution very approximate. This is in contrast to the climate spheres of the other azonal vegetation elements used in the reconstruction whose present-day distributions are well known, and which are therefore of higher resolution.

Because the source of some pollen grains may be distant from the central depression of the basin, this quantitative reconstruction of climatic parameters gives a regional wide-spread picture of the changes in moisture conditions rather than a local signal restricted to the Aral Sea and its nearest adjacent areas. To further constrain our climatic reconstruction, we compared the reconstructed values to modern instrumental data from Central Asia along the latitudinal gradient [40°75′–50°25′N] across the Aral Sea basin (Fig. 5).

Pollen zone P1 (10.75–9.97 m; ca. AD 0–400): basal arid interval

High values of the ratio Amaranthaceae–Chenopodiaceae/Poaceae concurrently with high frequency of steppe element *Artemisia* and Amaranthaceae–Chenopodiaceae indicate that prevailing climate from ca. AD 0 to 400 was colder and more arid than today, with mean annual temperatures of 4–6 °C, temperatures of the coldest month averaging –6 °C and mean annual precipitation never exceeding 300 mm/yr. The general feature of such climatic conditions is supported by sedimentological data and precipitation of gypsum interbedded with fine clays in the lowermost part of this zone. The transition between pollen zones P1 and P2 is probably characterized by a very short coring gap.

Pollen zone P2 (9.97–6.13 m; ca. AD 400–900): increasing humidity

Decreasing xeric conditions are inferred from low values of the ratio Amaranthaceae–Chenopodiaceae/Poaceae (<10) between ca. AD 400 and 900. Coevally, an increase in the abundance of warm-temperate elements and aquatic plants suggests that the climate became moderately moister and potentially warmer. Reconstructed climate conditions indeed document that mean annual precipitation fluctuated between 270 and 475 mm/yr, whereas temperatures of the warmest month averaged 21 °C (coldest month: –5 °C) and mean annual temperatures 9 °C. Increase in moisture conditions are concurrent with the evidence of lake-level rise, inferred from dinoflagellate cyst assemblages (Sorrel et al., 2006), and may have favoured the expansion of some riparian trees.

Pollen zone P3 (6.13–4.92 m; ca. AD 900–1150): strong aridification

This zone documents a return to strong arid conditions, as reflected by the progressive decrease in warm-temperate trees and the expansion of steppe elements *Artemisia* and Amaranthaceae–Chenopodiaceae. This is concurrent with high values of the aridity index (>10) and declined rainfall (200–230 mm/yr). Climate reconstruction document lower temperatures during this interval (coldest month: –7° to –10 °C; warmest month: 15°–21 °C; mean annual temperature: 4°–6 °C). Further evidence for a long-term aridification is provided by a gypsum layer at 4.86 m (Fig. 4).

Pollen zone P4 (4.92–2.02 m; ca. AD 1150–1450): increasing humidity

Increasing moisture conditions are inferred from a drop in the abundance of both steppe herbs and shrubs coincident with higher percentages of Poaceae and trees. Based on the ratio Amaranthaceae–Chenopodiaceae/Poaceae (<10), prevailing climate conditions were noticeably moister than at present. This is concurrent with enhanced precipitation (370–505 mm/yr). Reconstructed temperatures for this interval were higher (mean annual: 7°–11 °C; coldest month: –4 °C). Increasing moisture conditions are consistent with rising lake levels and important freshwater discharges in the Aral Sea, as indicated in the dinoflagellate cyst assemblages (Sorrel et al., 2006). Higher-water availability between ca. AD 1150 and 1450 probably favoured the expansion of trees onshore, with a possible development of a riparian association comprising warm-temperate trees (*Ulmus*, *Alnus*, *Populus*, *Corylus*) and maybe few mega-mesothermic elements (*Taxodium*-type, *Engelhardia*). The last sample records the onset of more arid conditions resulting in lower precipitation rates (<200 mm/yr).

Pollen zone P5 (2.02–0.00 m; ca. AD 1450–1980): brief aridification followed by present-day climate conditions

A third arid interval is recorded during ca. AD 1450–1550, as reflected by increasing abundance of steppe element *Artemisia* and slightly higher values of the ratio Amaranthaceae–Chenopodiaceae/Poaceae. This short phase is characterized by low precipitation rates (200–270 mm/yr) but more contrasting temperatures. Whereas both mean annual values (6°–9 °C) and temperatures for the warmest month (18.9°–20.5 °C) suggest warmer conditions in this interval, mean values for the coldest month decrease from –7 °C around AD 1450 to –9 °C at AD 1550. This interpretation is confirmed by sedimentological data, with precipitation of gypsum crystals in clay sediments around AD 1500. Reconstructed climatic parameters from the pollen content of surface sediments (AD 1550–1980) indicate contrasting precipitation rates (240–370 m/yr) and a slight warming trend (coldest month: –6° to –3 °C; warmest month: 20°–22 °C; mean annual temperature: 7 °C). Observations of present-day landscapes along the northern shore of the Aral Sea corroborate pollen evidence of enhanced aridity and higher

temperatures in recent decades. The reconstructed climate parameters in the uppermost sample (i.e., AD 1980) are in accordance with present-day instrumental data from Central Asia (Fig. 5), where mean annual temperature and precipitation respectively decrease/increase from 14 °C/110 mm at 40°75'N to 4 °C/310 mm at 50°25'N, validating the ranges of values obtained in our climate quantification. However, whether reconstructed temperature for the coldest month (−3 °C) fairly overlaps instrumental values (−1° to −16 °C), the estimated value for the warmest month (22 °C) appears slightly lower than the instrumental ones (22°–30 °C). An explanation for this could be the rapid warming trend observed during the past 20 yr, which is not documented in our pollen record.

Discussion and conclusions

Today, the climate in the deserts of Central Asia is mostly controlled by the shifts of the westerly cyclonic circulation and depends on the position of the Siberian High during winter and spring (Zavialov, 2005). In addition, local precipitation occurs during winter and early spring when depressions, developing over the eastern Mediterranean, subsequently move along a northeast trajectory where they may replenish moisture over the Caspian Sea (Létolle and Mainguet, 1993; Roberts and Wright,

1993; Aizen et al., 2001; Lioubimtseva, 2002). Therefore, we may expect elevated precipitation in Central Asia when moisture-transporting storms are stronger in the eastern Mediterranean region and, if so, we should find similar pattern of humidity between areas influenced by eastward moving storms (Israel, Turkey, Iran) and the Aral Sea basin during the last 2000 yr. Detailed palaeoclimatological studies based on $\delta^{18}\text{O}$ measurements from carbonate deposits of the Soreq Cave (Israel) (Schilman et al., 2002) provide a reliable record for comparison with the pollen-derived climate reconstruction presented here (Fig. 6). We also use the relative abundance of reworked dinoflagellate cysts, which is expected to increase during periods of elevated sheet wash from shore, as a further proxy of the rainfall intensity (Sorrel et al., 2006).

Whereas a cold and arid period (mean annual rainfall <300 mm) has been inferred from the pollen flora during AD 0–400, Schilman et al. (2002) document declining rainfall leading to dry events in Israel around AD 0. A similar phenomenon was reported in Syria, with reduced winter/spring rains (Bryson, 1996). Coevally, a decrease in lake level is reported from Lake Van in Turkey, evidencing a period of decreasing humidity between ca. 1500 BC and AD 0 (Landmann et al., 1996; Lemcke and Sturm, 1996). The decrease of rainfall is possibly related to a change in the mode of the North Atlantic Oscillation

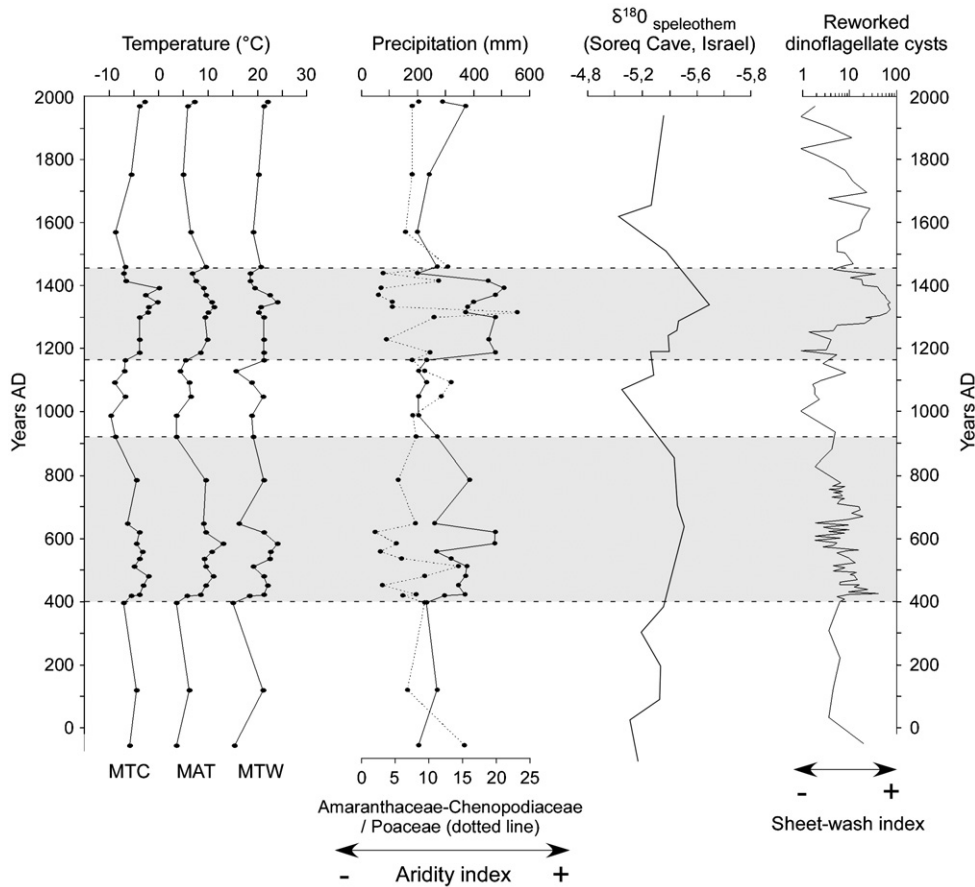


Figure 6. Comparison between reconstructed climate parameters (temperature, precipitation: black full lines) from section CH2/1, the $\delta^{18}\text{O}$ record from carbonate deposits in the Soreq Cave (Israel; Schilman et al., 2002) and the sheet wash index derived from the relative abundance of reworked dinoflagellate cysts at Chernyshov Bay (Sorrel et al., 2006). Grey shadings represent periods of increased temperature and rainfall in the Aral Sea basin when moisture-transporting storms are stronger from the Eastern Mediterranean Sea.

(NAO) that reduced cyclonic activity over the eastern Mediterranean, being high during a negative NAO mode (Hurrell, 1995; Hurrell et al., 2003). This is in accordance with Aizen et al. (2001), who found that the NAO has a statistically significant inverse relationship with moisture availability over mid-latitudes of continental Asia. Based on correlation analyses between atmospheric circulation patterns and regional precipitation, they reported that a negative (positive) difference in sea-level pressure anomalies between the Azores and the Iceland is favourable (unfavourable) for precipitation development over the middle plains of Asia.

Following this aridification, the time interval ca. AD 400–900 is characterized by some warmer and wetter climate conditions in the Aral Sea basin, which favoured the development of some arboreal vegetation in the less dry edaphic areas. This is supported by a conspicuous decrease in the $\delta^{18}\text{O}$ of carbonate deposits from the Soreq Cave (Schilman et al., 2002; Fig. 6), which infers elevated precipitation rates in Israel during AD 400–900 linked to stronger storms over the eastern Mediterranean. Other evidences document a period of maximum precipitation around AD 700, as inferred from land records including tree assemblages (Lipschitz et al., 1981), high-stand levels of the Dead Sea (Frumkin et al., 1991) and carbonate cave deposits in Israel (Bar-Matthews et al., 1998).

The period AD 900–1150 is characterized by a return to colder and more arid conditions in the Aral Sea basin concurrently with declining rainfall (<270 mm/yr) and low mean annual temperatures, suggesting lowered moisture derived from the eastern Mediterranean in winter and early spring during a possible positive phase of the NAO. This is in accordance with other palaeoenvironmental records from the eastern Mediterranean which document colder conditions and reduced precipitation between AD 850 and 1200 (Issar et al., 1991; Schilman et al., 2002).

After AD 1150, elevated moisture conditions during a warmer period are inferred with precipitation rates frequently beyond 400 mm/yr, although the associated change in the vegetation pattern was not registered in the C:N ratio (<10) of organic isotopes from Chernyshov Bay (Austin, unpublished data). It coincides, however, with elevated sheet wash from shore as reflected by higher abundance of reworked dinoflagellate cysts. A similar pattern to increasing humidity is inferred from lowered $\delta^{18}\text{O}$ values in speleothems from the Soreq Cave between AD 1200 and 1500 (Fig. 6), suggesting higher rainfall over the eastern Mediterranean region during the Medieval Warm Period. This event also corresponds to high-stand levels of the Dead Sea (Issar et al., 1991) and the Sea of Galilee (Frumkin et al., 1991).

A brief aridification occurred again during AD 1450–1550. This short-term change towards colder/drier conditions probably coincide with the Little Ice Age, whose signature has been previously recorded in $\delta^{18}\text{O}$ values from the foraminiferan *G. ruber* in the eastern Mediterranean Sea (Schilman et al., 2001) and in carbonate deposits from Israel (Bar-Matthews et al., 1998; Schilman et al., 2002). From AD 1550 onwards, increased temperatures document a progressive warming. For

the last 2000 yr, no human activity exerting control on vegetation change has been detected from the pollen record of Chernyshov Bay.

Despite a time-resolution of ca. 50 yr, the climate reconstruction provides compelling evidence that centennial-scale events are recorded during the last 2000 yr (Fig. 6). In the Aral Sea basin, climate conditions may fluctuate with a periodicity of ~400 yr, with intervals of relatively elevated moisture conditions alternating with more arid phases. Since our data match fairly well with the Soreq cave record from Israel (Schilman et al., 2002), we thus conclude that the precipitation pattern in the Aral Sea basin is directly linked to atmospheric changes in the eastern Mediterranean region, modulating moisture distribution towards the Middle East and Western Central Asia. This link may document a teleconnection to the NAO during negative phases. Modelling of Holocene climatic scenarios would improve our understanding of atmosphere–biosphere interactions in this vast arid region and identify important thresholds between climate changes and landscape responses.

Acknowledgments

The CLIMAN project was funded by INTAS (European Union) (Project No. Aral 00-1030), the German Science Foundation (DFG Project 436 RUS 111/663-OB 86/4) and NATO CLG Ref. 980445. We are grateful for this support. We wish to thank especially Dr. François Demory for excellent support in the field. The authors gratefully acknowledge Dr. Derek B. Booth and two anonymous reviewers for their constructive comments which have helped to improve the manuscript.

References

- Aizen, E.M., Aizen, V.B., Melack, J.M., Nakamura, T., Ohta, T., 2001. Precipitation and atmospheric circulation patterns at mid-latitudes of Asia. *International Journal of Climatology* 21, 535–556.
- Austin, P., Mackay, A., Palagushkina, O., Leng, M., 2007. A high-resolution diatom-inferred palaeoconductivity and sea-level record of the Aral Sea for the last ca. 1600 years. *Quaternary Research*. *Quaternary Research* 67, 383–393.
- Bar-Matthews, M., Ayalon, A., Kaufmann, A., 1998. Middle to late Holocene (6500 years period) palaeoclimate in the eastern Mediterranean region from stable isotopic composition of speleothems from Soreq Cave, Israel. In: Issar, A.S., Brown, N. (Eds.), *Water, Environment and Society in Time of Climate Change*. Kluwer Academic Publishers, pp. 203–214.
- Boomer, I., Aladin, N., Plotnikov, I., Whatley, R., 2000. The palaeolimnology of the Aral Sea: a review. *Quaternary Science Reviews* 19, 1259–1278.
- Boroffka, N.G.O., Oberhänsli, H., Achatov, G.A., Aladin, N.V., Baipakov, K.M., Erzhanova, A., Hoernig, A., Krivonogov, S.K., Lobas, D.A., Savel'eva, T.V., Wuennemann, B., 2005. Human settlements on the northern shores of Lake Aral and water level changes. *Mitigation and Adaptation Strategies for Global Change* 10, 71–85.
- Boroffka, N.G.O., Oberhänsli, H., Sorrel, P., Demory, F., Reinhardt, C., Wuennemann, B., Alimov, K., Baratov, S., Rakhimov, K., Saparov, N., Shirinov, T., Krivonogov, S.K., 2006. Archaeology and climate: Settlement and lake level changes at the Aral Sea. *Geoarchaeology* 21 (7), 721–734.
- Bortnik, V.N., Chistyeva, S.P. (Eds.), 1990. *Hydrometeorology and Hydrochemistry of the USSR Seas. The Aral Sea, vol. VII. Gidrometeoizdat, Leningrad*. 196 pp. (in Russian).

- Bronk Ramsey, C., 2005. OxCal version 3.10.
- Bryson, R.A., 1996. Proxy indications of Holocene winter rains in southwest Asia compared with simulated rainfall. In: Dalfes, H.N., Kukla, G., Weiss, H. (Eds.), *Third Millennium BC; Climate Change and Old World Collapse*. NATO ASI Series I, vol. 49. Springer Verlag, pp. 465–473.
- Cour, P., 1974. Nouvelles techniques de détection des flux et de retombées polliniques: étude de la sédimentation des pollens et des spores à la surface du sol. *Pollen et Spores* 23 (2), 247–258.
- Cour, P., Duzer, D., 1978. La signification climatique, édaphique et sédimentologique des rapports entre taxons en analyse pollinique. *Annales des Mines de Belgique* 7/8, 155–164.
- Cour, P., Zheng, Z., Duzer, D., Calleja, M., Yao, Z., 1999. Vegetational and climatic significance of modern pollen rain in northwestern Tibet. *Review of Palaeobotany and Palynology* 104, 183–204.
- El Moslimany, A.P., 1990. Ecological significance of common non-arboreal pollen: examples from drylands of the Middle East. *Review of Palaeobotany and Palynology* 76 (2–4), 343–350.
- Esper, J., Schweingruber, F.H., Winiger, M., 2002. 1300 years of climate history for Western Central Asia inferred from tree-rings. *Holocene* 12, 267–277.
- Frumkin, A., Magaritz, M., Carmi, I., Zak, I., 1991. The Holocene climatic record of the salt caves of Mount Sedom, Israel. *Holocene* 1, 191–200.
- Guiot, J., 1987. Late Quaternary climatic change in France estimated from multivariate pollen time series. *Quaternary Research* 28, 100–118.
- Guiot, J., 1990. Methodology of the last climatic cycle reconstruction in France from pollen data. *Palaeogeography, Palaeoclimatology, Palaeoecology* 80, 49–69.
- Heim, C., 2005. Die Geochemische Zusammensetzung der Sedimente im Aralsee und Sedimentationsprozesse während der letzten 100 Jahre. Diploma thesis, Alfred-Wegener-Institut Bremerhaven, 89 pp.
- Hurrell, J., 1995. Decadal trends in the North Atlantic Oscillation—Regional temperatures and precipitation. *Science* 269, 676–679.
- Hurrell, J., Kushnir, Y., Ottersen, G., Visbeck, M., 2003. An overview of the North Atlantic Oscillation. In: Hurrell, J., Kushnir, Y., Ottersen, G., Visbeck, M. (Eds.), *The North Atlantic Oscillation: Climatic Significance and Environmental Impact*. AGU, Washington, pp. 1–35.
- Issar, A.S., Govrin, Y., Geyh, A.M., Wakshal, E., Wolf, M., 1991. Climate changes during the Upper Holocene in Israel. *Israelian Journal Earth Sciences* 40, 219–223.
- Klotz, S., 1999. Neue Methoden der Klimarekonstruktion—angewendet auf quartäre Pollensequenzen der französischen Alpen. *Tübinger Mikropaläontologische Mitteilungen* 21, 169 pp.
- Klotz, S., Pross, J., 1999. Pollen-based reconstructions in the European Pleistocene: the modified indicator species approach as a tool for quantitative analysis. *Acta Palaeobotanica, Supplementum* 2, 481–486.
- Klotz, S., Guiot, J., Mosbrugger, V., 2003. Continental European Eemian and early Würmian climate evolution: comparing signals using different quantitative reconstruction approaches based on pollen. *Global and Planetary Change* 36, 277–294.
- Klotz, S., Müller, U., Mosbrugger, V., de Beaulieu, J.L., Reille, M., 2004. Eemian to early Würmian climate dynamics: history and pattern of changes in Central Europe. *Palaeogeography, Palaeoclimatology, Palaeoecology* 211, 107–126.
- Kremenetski, C.-V., Tarasov, P.E., 1997. Postglacial development of Kazakhstan pine forests. *Géographie Physique et Quaternaire* 51 (3), 391–404.
- Kremenetski, C.-V., Tarasov, P.E., Cherkinsky, A.E., 1997. The latest Pleistocene in Southwestern Siberia and Kazakhstan. *Quaternary International* 41/42, 125–134.
- Landmann, G., Reimer, A., Lemcke, G., Kempe, S., 1996. Dating Late Glacial abrupt climate changes in the 14,570-yr long continuous varve record of Lake Van, Turkey. *Palaeogeography, Palaeoclimatology, Palaeoecology* 122, 107–118.
- Lemcke, G., Sturm, M., 1996. ^{18}O and trace element measurements as proxy for the reconstruction of climate changes at Lake Van (Turkey). In: Dalfes, H.N., Kukla, G., Weiss, H. (Eds.), *Third Millennium BC; Climate Change and Old World Collapse*. NATO ASI Series I, vol. 49. Springer Verlag, pp. 653–678.
- Létolle, R., Mainguet, M., 1993. *Aral*. Springer Verlag, Paris, 358 pp.
- Lioubimtseva, E., 2002. Arid environments. In: Shahgedanova, M. (Ed.), *Physical Geography of Northern Eurasia*. Oxford University Press, Oxford, 571 pp.
- Lioubimtseva, E., Cole, R., Adams, J.M., Kapustin, G., 2005. Impacts of climate and land-cover changes in arid lands of Central Asia. *Journal of Arid Environments* 62, 285–308.
- Lipschitz, N., Lev-Yadun, S., Waisel, Y., 1981. Dendroarchaeological investigations in Israel (Asada). *Israel Exploration Journal* 31, 230–234.
- Mosbrugger, V., Utescher, T., 1997. The coexistence approach—A method for quantitative reconstructions of Tertiary terrestrial palaeoclimate data using plant fossils. *Palaeogeography, Palaeoclimatology, Palaeoecology* 134, 61–86.
- New, M., Hulme, M., Jones, P., 1999. Representing twentieth century space-time climate variability. I: development of a 1961–1990 mean monthly terrestrial climatology. *Journal of Climate* 12, 829–856.
- Nezlin, N.P., Kostianoy, A.G., Li, B.-L., 2005. Inter-annual variability and interaction of remote-sensed vegetation index and atmospheric precipitation in the Aral Sea region. *Journal of Arid Environments* 62, 677–700.
- Nourgaliev, D.K., Heller, F., Borisov, A.S., Hajdas, I., Bonani, G., Iassonov, P.G., Oberhänsli, H., 2003. Very high resolution paleosecular variation record for the last 1200 years from the Aral Sea. *Geophysical Research Letters* 30 (17), 4-1–4-4.
- Peyron, O., Guiot, J., Cheddadi, R., Tarasov, P., Reille, M., de Beaulieu, J.L., Bottema, S., Andreu, V., 1998. Climate reconstruction in Europe for 18,000 yr B.P. from pollen data. *Quaternary Research* 49, 183–196.
- Prentice, I.C., Cramer, W., Harrison, S.P., Leemans, R., Monserud, R.A., Solomon, A.M., 1992. A global biome model based on plant physiology and dominance, soil properties and climate. *Journal of Biogeography* 19, 117–134.
- Prentice, I.C., Guiot, J., Huntley, B., Jolly, D., Cheddadi, R., 1996. Reconstructing biomes from palaeoecological data: a general method and its application to European pollen data at 0 and 6 ka. *Climate Dynamics* 12, 185–194.
- Reimer, P.J., Baillie, M.G.L., Bard, E., Bayliss, A., Beck, J.W., Bertrand, C.J.H., Blackwell, P.G., Buck, C.E., Burr, G.S., Cutler, K.B., Damon, P.E., Lawrence Edwards, R., Fairbanks, R.G., Friedrich, M., Guilderson, T.P., Hogg, A.G., Hughen, K.A., Kromer, B., McCormac, G., Manning, S., Bronk Ramsey, C., Reimer, R.W., Remmele, S., Southon, J.R., Stuiver, M., Talamo, S., Taylor, F.W., van der Plicht, J., Weihsenmeyer, C.E., 2004. IntCal04 terrestrial radiocarbon age calibration, 0–26 cal. yr BP. *Radiocarbon* 46 (3), 1029–1058.
- Roberts, N., Wright, H.E., 1993. Vegetational, lake-level, and climatic history of the Near East and Southwest Asia. In: Wright, H.E. (Ed.), *Global Climates since the Last Glacial Maximum*. University of Minnesota Press, pp. 194–220.
- Rubanov, I.V., Ischniyanov, D.P., Baskakova, M.A., 1987. *Geology of the Aral Sea*. Tashkent, 248 pp. (in Russian).
- Schilman, B., Bar-Matthews, M., Almogi-Labin, A., Luz, B., 2001. Global climate instability reflected by Eastern Mediterranean marine records during the Late Holocene. *Palaeogeography, Palaeoclimatology, Palaeoecology* 176, 157–176.
- Schilman, B., Ayaly, A., Bar-Matthews, M., Kagan, E.J., Almogi-Labin, A., 2002. Sea-land palaeoclimate correlation in the Eastern Mediterranean region during the Late Holocene. *Israel Journal of Earth Sciences* 51, 181–190.
- Seredkina, E.A., 1960. Dust storms in Kazakhstan (Pyl'nie buri v Kazakhstane). *Proceedings of KazNIGMI* 15, 54–59 (in Russian).
- Sorrel, P., Popescu, S.-M., Head, M.J., Suc, J.P., Klotz, S., Oberhänsli, H., 2006. Hydrographic development of the Aral Sea during the last 2000 years based on a quantitative analysis of dinoflagellate cysts. *Palaeogeography, Palaeoclimatology, Palaeoecology* 234 (2–4), 304–327.
- Tarasov, P.E., 1992. *Holocene palaeogeography of the steppe zone of Northern and Central Kazakhstan*. Thesis, Moscow University, 213 pp.
- Tarasov, P.E., Jolly, D., Kaplan, J.O., 1997. A continuous Late Glacial and Holocene record of vegetation changes in Kazakhstan. *Palaeogeography, Palaeoclimatology, Palaeoecology* 136, 281–292.
- Tarasov, P.E., Webb III, T., Andreev, A.A., Afanas'eva, N.B., Berezina, N.A., Bezusko, L.G., Blyakharchuk, T.A., Bolikhovskaya, N.S., Cheddadi, R., Chernavskaya, M.M., Chernova, G.M., Dorofeyuk, N.I., Dirksen, V.G.,

- Elina, G.A., Filimonova, L.V., Glebov, F.Z., Guiot, J., Gunova, V.S., Harrison, S.P., Jolly, D., Khomutova, V.I., Kvavadze, E.V., Osipova, I.M., Panova, N.K., Prentice, I.C., Saarse, L., Sevastyanov, D.V., Volkova, V.S., Zernitskaya, V.P., 1998a. Present-day and mid-Holocene biomes reconstructed from pollen and plant macrofossil data from the former Soviet Union and Mongolia. *Journal of Biogeography* 25, 1029–1053.
- Tarasov, P.E., Cheddadi, R., Guiot, J., Bottema, S., Peyron, O., Belmonte, J., Ruiz-Sanchez, V., Saadi, F.A., Brewer, S., 1998b. A method to determine warm and cool steppe biomes from pollen data; application to the Mediterranean and Kazakhstan regions. *Journal of Quaternary Sciences* 13, 335–344.
- Van Campo, E., Cour, P., Sixuan, H., 1996. Holocene environmental changes in Bangong Co Basin (Western Tibet). Part 2: The pollen record. *Palaeogeography, Palaeoclimatology, Palaeoecology* 120, 49–63.
- Velichko, A.A., 1989. The relationship of the climatic changes in the high and low latitudes of the Earth during the Late Pleistocene and Holocene. In: Velichko, A.A., et al. (Ed.), *Paleoclimates and Glaciation in the Pleistocene*. Nauka Press, Moscow, pp. 5–19.
- Zavialov, P.O., 2005. *Physical oceanography of the dying Aral Sea*. Springer Verlag, published in association with Praxis Publishing, Chichester, UK, 146 pp.